Sorptivity and acid resistance of ambient-cured geopolymer mortars containing nano-silica

Partha Sarathi Deb[a]*, Prabir Kumar Sarker[b], Salim Barbhuiya[c]

[a] PhD student, Department of Civil Engineering, Curtin University, GPO Box U1987, Perth, WA 6845, Australia

[b] Senior Lecturer, Department of Civil Engineering, Curtin University, GPO Box U1987, Perth, WA 6845, Australia

[c] Lecturer, Department of Civil Engineering, Curtin University, GPO Box U1987, Perth, WA 6845, Australia

*Tel | +61 8 9266 7568; Fax | +61 8 9266 2681 email: partha.deb@postgrad.curtin.edu.au

Abstract

This study investigated the effects of nano-silica on flowability, strength development, sorptivity and acid resistance properties of fly ash geopolymer mortars cured at 20^{o}C. The changes in mass, compressive strength and microstructure of the specimens after immersion in acid solutions for different durations were determined. The microstructures were studied by scanning electron microscopy (SEM), energy dispersive spectroscopy (EDS) and X-ray diffraction (XRD) analysis. It was found that addition of nano-silica in geopolymer mortars based on fly ash alone or fly ash blended with 15% GGBFS or 10% OPC improved the compactness of microstructure by reducing porosity. Thus, the nano-silica reduced sorptivity and increased compressive strength of the mixes. The average mass loss after 90 days of immersion in acid solutions reduced from 6.0% to 1.9% by addition of 2% nano-silica. Similarly, significant reduction in strength loss after immersion in acid solution was observed in the specimens by using nano-silica.

Keywords: A*cid resistance; ambient curing*; *fly ash; geopolymer; nano-silica; sorptivity*

1. Introduction

Works on the development of geopolymer binder as an alternative to traditional cement has been considerably increased in the recent years. This is because of the numerous benefits of geopolymers over traditional cement binder such as lower CO_2 emission [1], requirement for less processing of the raw materials [2] and development of desired strength and structural

properties [3, 4, 5]. Geopolymerization is a process where the glassy constituents of the aluminosilicate source materials are transformed into a compact binder [6]. Several factors such as reactivity of the source materials [7], curing temperature, alkaline activator to source material ratio [3, 8, 9] and the type of alkaline activator play important roles in the geopolymerization process. Selection of the binder compositions is an important factor affecting the properties of fresh and hardened geopolymers [8, 9]. Geopolymers based on low-calcium fly ash cured at ambient temperature takes very long time to set and it develops relatively low strength as compared to those cured at elevated temperature such as at 60 ^{o}C. Previous studies [3, 9] showed that the setting and strength development of low-calcium fly ash geopolymers can be improved by a small percentage of ground granulated blast furnace slag (GGBFS) or ordinary Portland cement (OPC) in the binder.

Improvements in the mechanical properties of a cementitious matrix by the addition of nano materials were reported by numerous studies [10-13]. It was observed that a small percentage of nano-silica in the cementitious system can result in a considerable strength improvement with a denser microstructure. However, the performance of nano-silica in cementitious materials is dependent on its morphology, method of preparation and its uniform dispersion in the mixture [14, 15]. It was reported by Adak et al. [16] that addition of 6% nano-silica increased compressive strength of fly ash geopolymers. Gao et al. [17] showed that nano-silica increased the strength of alkali activated slags. These studies focused on the improvements of strength properties of alkali activated binders by using nano-silica. Studies on the durability of fly ash geopolymers in aggressive chemical environment are scarce in literature. Especially, it is necessary to study if the durability properties of geopolymers can be improved by using nano-silica. Concrete structures are often exposed to acidic environment such as in ground water, industrial effluents and acid rains. Therefore, acid resistance of concrete is an important property for its performance in aggressive environment.

Mehta [18] observed that acid attack on a cementitious binder caused decalcification and formation of soluble products. Chindaprasirt et al. [19] noted that the high strength loss by the acid exposure of alkali activated fly ash-silica fume composites was due to the low initial strength of the mortar and the favourable dissolution of excess silica in the acid solution. However, Bakharev [20] observed better resistance of geopolymers than OPC binders in exposure to aggressive environment. Breck [21] noted that polymer structures with a Si/Al ratio of 1 are more easily attacked by the acid than more siliceous polymers. Ismail et al. [22] found that the H^{+} from H_2SO_4 ionization could destroy the alumino-silicate network

in geopolymer and yielded silicic acid ($Si(OH)_4$) and aluminium ions (Al^{3+}) from the gel polymer.

It was shown that addition of nano-silica in OPC or other cementitious binders significantly enhanced the compressive strength along with its durability properties. Addition of a small percentage of nano-silica could be a potential way to improve the strength and durability properties of low-calcium fly ash geopolymers cured at ambient temperature. Thus a comprehensive study is required to understand the possible beneficial effects of nano-silica in fly ash geopolymers cured at room temperature. This study investigated the effects of the addition of 0-3% nano-silica on the flowability, strength and porosity of geopolymer mortars based on fly ash only and fly ash blended with GGBFS or OPC. The durability properties such as sorptivity and resistance to acid were studied by determining the changes in mass and strength after immersion in an acid solution. The microstructural changes were studied by using SEM, EDS and XRD analysis to obtain an insight into the observed strength and durability properties.

2. Experimental work

2.1. Materials

Low-calcium fly ash was used as the main aluminosilicate source for all geopolymer mortars. Commercially available GGBFS and OPC were blended with fly ash to accelerate the setting of geopolymers for curing at room temperature. Commercially available nano-silica (NS) with average particle diameter of 15 nm was used as an additive to improve the properties of fresh and hardened properties of geopolymer mortars. The chemical compositions of these materials are given in Table 1. The blaine's fineness of the regular fly ash, OPC and GGBFS were 340 m^2/kg, 370 m^2/kg and 450 m^2/kg respectively.

The activating chemicals were sodium silicate with a chemical composition of (wt. %): Na_2O = 11.5, SiO_2 = 30.0 and water = 58.5, and 8M sodium hydroxide solution prepared from analytical grade sodium hydroxide pellets. The fine aggregate was natural sand with a nominal maximum size of 1.18 mm.

2.2. Geopolymer mixtures

The mix proportions of geopolymer mortars were designed taking the final unit weight as 2200 kg/m^3.The composition of the geopolymer mortar mixtures were calculated based on the authors' previous works [3, 4, 15] on geopolymers cured at room temperature. The mix proportions are given in Table 2. The mixtures are classified into three groups named as fly ash only, GGBFS blended fly ash and OPC blended fly ash series. Mixture FA-NS0, without

nano-silica, was the control mixture designed with fly ash alone as the binder for the fly ash-only geopolymer series. Similar control mixtures were prepared for GGBFS (FA-S-NS0) and OPC (FA-PC-NS0) blended fly ash geopolymer mortars. The mixtures are designated based on the constituents of the binder. For example, the designation FA-S-NS3 represents a geopolymer mixture having 3% nano-silica (NS) in the GGBFS (S) blended fly ash (FA) geopolymer mortar. The percentages of GGBFS and OPC were fixed at 15% and 10% of the binder respectively. The binder to alkaline liquid ratio and the molarity of NaOH were fixed at 0.4 and 8M respectively. These proportions were used based on authors' previous studies [3, 8, 9].

2.3. Mixing of geopolymer mortars and the test methods

The alkaline activator was a combination of sodium silicate and sodium hydroxide solutions with a mass ratio of 2.0. The nano-silica particles were dispersed in the silicate solution by using ultra-sonication prior to mixing of the mortar [15]. The fly ash and the fine aggregates were first mixed together in a Hobart mixer. This was followed by addition of the activator solution to the dry materials. The mixing was then continued further for about 3-5 minutes to produce fresh geopolymer mortar. Flow test of fresh geopolymer mortar was conducted in accordance with ASTM C1437-13 standard [23]. Cube mortar specimens of size 50 × 50 × 50 mm were cast for compressive strength tests and 100 × 50 mm cylinder specimens were cast for sorptivity tests. The specimens were demolded at 24hrs after casting and then cured at room temperature (20±2°C) at a relative humidity of 70±10%. Compressive strength tests of the specimens were performed at 7, 28, 56 and 90 days in accordance with the ASTM C109 [24] Standard.

The morphology of the hardened samples was examined by a MIRA3 TESCAN using a scanning electron microscope (SEM). X-ray diffraction (XRD) experiments were conducted on a Siemens D500 Bragg–Brentano diffractometer in a 2h-range of 5–80Θ. Operating conditions for the XRD were set a 40 kV and 30 mA using a Cu ka X-ray source. Crystalline phases of the geopolymers were identified by comparison with a Powder Diffraction File (PDF).

Resistance to sulfuric acid was determined by the modified test method B of the ASTM C 267 Standard [25]. The geopolymer cube mortar specimens were fully immersed in 3% sulfuric acid solution at the age of 28 days for 12 consecutive weeks. The acid solution was replaced weekly and the pH level was monitored regularly to maintain the designated pH of 3.0.The specimens were removed from the acid solution after the exposure period and brushed carefully to remove the loose particles from its surface. They were then left for

drying under room temperature for 1hr before recording the mass changes. Strength and microstructure of the geopolymer specimens were also investigated after different exposure periods. Sorptivity tests were conducted with 100 mm diameter and 50 mm height specimens in accordance with ASTM C1585-13 [26]. The sides of the specimens were coated with epoxy to allow free water movement only through the bottom face.

3. Results and discussion

3.1. Flow behaviour of fresh geopolymer mortar

The effects of the percentage of nano-silica on the flow of fresh geopolymer mortars are shown in Fig. 1. It can be seen that the flow values of the mixes containing GGBFS and OPC were less than those of the fly ash only mixes. The decrease in flow is because of the early reaction of the calcium contained in GGBFS and OPC. The trend is similar to the observations in previous works [3, 4, 8, 9]. Nath and Sarker [9] and Provis et al. [27] reported that the flow of fly ash geopolymer mortars decreased with the increase of calcium bearing components in the binder. Gao et al. [17] noted that lower slag content provided a better flowability due to their morphological differences. It can be seen from Fig.1 that the flow of geopolymer mortars gradually decreased with the increase of nano-silica. The flow of fly ash only geopolymer mortars decreased from 135% (FA-NS0) to 115% (FA-NS3) with the addition of 3% nano-silica. The flow decreased from 98% to 64% by the addition of 3% nano-silica in the GGBFS blended fly ash geopolymer mortar. Similarly, flow decreased from 80% to 50% by 3% nano-silica in the OPC blended fly ash geopolymer mortar. The decrease of flow in the mixes of all three series by the inclusion of nano-silica is attributed to the increased liquid demand and accelerated reaction because of its high specific surface. The geopolymer mortars based on GGBFS and OPC blended fly ash containing 3% nano-silica were relatively stiff in nature and showed low workability.

3.2. Compressive strength

The compressive strength developments of the fly ash geopolymer mortars with 0%, 1%, 2% and 3% nano-silica are shown in Fig. 2. Each value is an average of the results obtained from 3 identical specimens. The coefficients of variation of the results were mostly within 5%. For example, the coefficients of variation of the 28 day-compressive strengths all the geopolymer mixtures were in the range of 0.38% to 5.1%.

It can be seen from the figure that the rate of strength development slowed down significantly after 28 days and it was negligible after the age of 56 days. Noticeable increase of strength can be seen in the fly ash geopolymer mixtures containing nano-silica. The extent of the increase in strength is dependent on the percentage of nano-silica. The highest strengths at all ages up to 90 days were found in the mixes with 2% nano-silica. While the strength of the mix with 3% nano-silica was higher than that of the control mix (FA-NS0), it was less than that of the mix with 2% nano-silica. Fernandez and Palomo [28] reported that the fineness of the source material played an important role in the strength development of geopolymer binders. Temuujin et al. [29] also showed that the reduction of particle size and change in morphology increase the dissolution rate which eventually increased the compressive strength of geopolymer binder.

It was shown in previous works [3, 8, 9] that curing temperature, molarity of sodium hydroxide and the reactivity of the source materials played crucial roles on the strength development of fly ash geopolymers. Generally, geopolymers based on fly ash only and cured at room temperature showed low compressive strength because of the slow geopolymerization process. The strength development in the specimens of the mixes without nano-silica showed similar trend in Fig.2. The nano-silica takes part in the reaction process from an early age because of its high specific surface. A greater degree of reaction of the aluminosilicate source materials is expected to give higher strength [30]. However, the results of this study suggest that there is a limiting value on the percentage of nano-silica beyond which no further strength increase is obtained. Thus, the optimum dosage of nano-silica for this mix series is found to be 2%. Belkowitz et al. [31] noted that the unreacted nano-silica caused an excessive self-desiccation and cracking in the matrix that eventually reduced the strength. Therefore, the less strength of the mix with 3% nano-silica than that of the mix with 2% nano-silica is attributed to the presence of unreacted particles acting as defect sites.

The strength developments of OPC and GGBFS blended series with the different amounts of nano-silica are shown in Figs. 3 and 4. As mentioned earlier, low-calcium fly ash was blended with either 10% OPC or 15% GGBFS in order to accelerate the setting of these mixes. As other ingredients remained constant, Figs. 3 and 4 show the influence of nano-silica addition on the strength development.

It is noteworthy that inclusion of nano-silica from 0 to 3% in the OPC and GGBFS blended series increased compressive strength by 40 to 64% as compared to the corresponding control mixes. Chindaprasirt et al. [32] and Somna et al. [33] reported that larger surface area of the source materials increased the geopolymerization process and

eventually increased the strength. It is noted from Fig.4 that mixes with 1%, 2% and 3% nano-silica, in the OPC blended series exhibited 41%, 63% and 50% higher strength respectively than the mix without nano-silica. Similar trend was also observed for GGBFS blended geopolymer mortars. The pore refinement process of nano-silica has resulted in higher strength of the geopolymer mixes. The addition of nano-silica increases the supply of the Si required for the geopolymerization process. It is noteworthy that due to its very large specific surface, nano-silica is highly reactive as compared to that of other cementitious materials such as fly ash, OPC and GGBFS. The main effect of the nano-silica addition in OPC and GGBFS blended series was the acceleration of the interconnected structure growth due to higher geopolymerization process that eventually resulted in higher compressive strength. The effect of nano-silica on strength development was similar in all the three series of mixes and the optimum percentage of nano-silica was found as 2%.

3.3. Sorptivity

Sorptivity tests were conducted for the mortar mixes without nano-silica and with 2% nano-silica. Nano-silica dosage of 2% was selected for the sorptivity and acid resistance tests since this percentage was found to maximise the compressive strength. The sorptivity coefficients of the fly ash only, OPC and GGBFS blended fly ash geopolymer mortars are given in Fig.5. As shown by the results, sorptivity coefficient of the mixes without nano-silica was in the range of 3.575×10^{-3} mm/s$^{1/2}$ to 3.980×10^{-3} mm/s$^{1/2}$ and that of the mixes with 2% nano-silica was in the range of 1.247×10^{-3} mm/s$^{1/2}$ to 2.157×10^{-3} mm/s$^{1/2}$. Thus, it is apparent from the results that the sorptivity coefficient decreased with 2% nano-silica in the mortar mixes of all the three series. For example, sorptivity coefficient decreased from 3.575×10^{-3} mm/s$^{1/2}$ to 1.247×10^{-3} mm/s$^{1/2}$ by 2% nano-silica in the fly ash only geopolymer mortar. Sorptivity reduced by nano-silica in the GGBFS and OPC blended fly ash geopolymer mortars in a similar way. The decrease in sorptivity of the specimens indicates a reduction in the porosity by inclusion of nano-silica. The effect of nano-silica on the improvement of porosity is attributed to two reasons. Firstly, the particle packing of nano-silica in the wide distribution of binder particle sizes resulted in a denser matrix. Secondly, the reaction of nano-silica in geopolymerization process produced further amount of aluminosilicate gel along with the reaction products from the main source materials. It is likely that additional reaction product precipitated in the available pore structures. As described by Law et al. [34], an increase in SiO_2 increases the density of the matrix. Therefore, the combined filling effect of nano-silica by the improved particle packing and the additional reaction product produced a denser

binding matrix that reduced the porosity and increased compressive strength as seen in Figs. 2 to 4.

3.4 Resistance to attack by sulfuric acid

3.4.1. Change in mass

The geopolymer mortar specimens were immersed in 3% sulfuric acid solution for 90 days and the changes in mass were determined on a weekly basis. The change in mass of a specimen was calculated by comparing mass measured after exposure to acid solution to the initial mass before the exposure. The specimens were visually inspected for any deterioration by the exposure to acid solution. Photographs of the specimens without and with 2% nano-silica after 90 days immersion in the acid solution are shown in Fig.6. Photographs of the specimens before acid exposure are also shown in this figure for comparison. Generally, some minor erosion could be observed in all the specimens by the acid attack. Also, there were relatively more damages, especially at the corners of specimens without nano-silica and those containing OPC and GGBFS.

Changes in mass for specimens of all the geopolymer mixes are presented in Fig 7. The results show that mass of the geopolymer specimens gradually decreased with exposure time. It can be seen that the mass loss after 90 days of acid exposure for fly ash only geopolymer mix without nano-silica was 5.41% as compared to 1.9% for the mix with 2% nano-silica. After the same exposure period, the mass loss of the OPC blended fly ash geopolymer mixes without nano-silica (FA-PC-NS0) and with 2% nano-silica (FA-PC-NS2) were 6.0% and 2.3% respectively. Similarly, the 90-day mass losses for the GGBFS blended fly ash geopolymer mortars were 5.8 % without nano-silica (FA-S-NS0) and 1.5% with 2% nano-silica (FA-S-NS2). Overall, the mass loss varied from 1.9% to 6.00% for all the geopolymer mixes. These mass losses of the nano-silica incorporated fly ash geopolymer mortars are very small as compared to the mass losses usually shown by OPC based cementations materials [35, 36]. Previous studies [36, 37] on OPC based binders showed that sulfuric acid has a highly deleterious effect on mass loss. This is because sulfuric acid causes decomposition of the $Ca(OH)_2$ and forms gypsum that deteriorates the matrix by scaling and softening. Though the penetration of sulfuric acid can be reduced, the formation of gypsum in the regions close to the surface causes progressive disintegration of the matrix [37]. Therefore, the mass losses observed in the geopolymer specimens without nano-silica were much smaller than that can be expected in OPC based binders under the same exposure condition. However, addition of

2% nano-silica has further reduced the mass loss of geopolymer specimens. The effect of nano-silica on the changes in strength and microstructures by the exposure to sulfuric acid are studied in the following sections.

3.4.2. Change in compressive strength

The 28-day compressive strength of each geopolymer mix before exposure to acid solution is used as a benchmark to calculate the strength loss after each exposure period of 28, 56 and 90 days. The compressive strengths of the mortar specimens from 6 mixes are presented in Fig. 8. It can be seen from the figure that loss of strength occurred in all the geopolymer mixes and it increased with the increase of exposure period. It is noteworthy from Fig.8 that fly ash only, OPC and GGBFS blended fly ash geopolymer specimens without nano-silica exhibited higher strength loss as compared to those with nano-silica. The strength loss in the specimens without nano-silica ranged from 30% to 41% while that in the specimens with nano-silica ranged from 9% to 11%. For example, the strength value of mix FA-NS2 (2% nano-silica) after 90 days of sulfuric acid exposure was 54.0 MPa, as compared to 60.0 MPa prior to acid exposure. Whereas, the compressive strength of mix FA-NS0 (0% nano-silica) reduced from 29.0 MPa to 19.1 MPa after 90 days of immersion in sulfuric acid. Bakharev [20] showed that depolymerisation of the aluminosilicate polymers in acidic media resulted in a significant strength loss of alkali activated binders. Chindaprasirt [38] noted that the oxy-aluminium bridge (–Al–Si–O) of geopolymeric gel probably gets destroyed in acidic environment and leads to strength reduction of alkali activated binders. Reduction of permeability helps reduce the ingress of acid in to geopolymer matrix and thus improves the resistance to acid attack [35]. It is apparent from Fig.8 that incorporation of 2% nano-silica in fly ash based geopolymer can effectively reduce the rate of acid attack expressed in terms of strength loss. Belkowitz et al. [31] noted that the pore refinement process by nano-silica usually prevents the passage of aggressive elements into the deeper layers of hydrated gel structure. It means that the optimum amount of nano-silica present in the geopolymer mixes produces a denser structure that reduces the degradation by an acid. The results of the present study are also supported by the findings of Fattuhi and Hughes [36], and Israel et al. [37] that the lower porosity improved the acid resistance of hydrated gel.

Also, as expected, the strength loss in OPC blended fly ash based geopolymer mortar without nano-silica is greater than that of with 2% nano-silica incorporated samples (FA-PC-NS2). The strength loss reduced from 11.5 MPa (FA-PC-NS0) to 6.5 MPa (FA-PC-NS2) by 2% nano-silica in the OPC blended geopolymer mix (Fig.8). This highlights the poor

resistance of mix FA-PC-NS0 (without nano-silica) against a highly corroding and aggressive environment as compared to mix FA-PC-NS2 (with nano-silica). Incorporation of 2% nano-silica leads to a denser and less permeable pore structure prolonging the negative effects of acid attack. This observations correlates well with the findings of Hartman and Fogler [39] which showed that the increased amount of soluble silica produces a denser layer and helps to reduce the extent of damage in the aluminosilicate structure with the removal of each of the aluminium atoms under acid attack.

Similarly, In the GGBFS blended mix, the strength loss after 90 days of immersion reduced from 7.5 MPa (FA-S-NS0) to 4.0 MPa (FA-S-NS2) by 2% nano-silica. The results of this study show that inclusion of 2% nano-silica in all geopolymer series made a significant improvement in the strength loss as compared to that of the mix without nano-silica.

3.4.3. Change in microstructure

The SEM images of the fly ash only, OPC and GGBS blended fly ash based geopolymer mortars with and without nano-silica after 90 days exposure to sulfuric acid are presented in Figs. 9(a) to 9(f). Images of the specimens before acid exposure are also shown in the figure. Significant differences in microstructure were observed in all the specimens after 90 days of sulfuric acid exposure. It can be seen that the relatively compact microstructure of geopolymers before the acid exposure became more porous after the exposure to sulphuric acid. However, geopolymer mortar with nano-silica showed less deterioration than the fly ash geopolymer mortar without nano-silica. It is noted from Fig 9(a) that fly ash only geopolymer mortar without nano-silica (FA-NS0) immersed in sulfuric acid for 90 days exhibited porous and disintegrated gel clusters (point 2) around the unreacted particles (point 1). Similar observations can also be noted in the microstructures of the OPC and GGBFS blended fly ash geopolymer mortars. More compact and less porous structures can be observed in the mixes with nano-silica when comparisons are made between the microstructure of Fig. 9(d) to that in Fig. 9(c) and the microstructure of Fig. 9(e) to that in Fig. 9(f). Bakharev [20] pointed out that disintegration of microstructure along with significant loss of strength in geopolymer materials is due to low inter crystalline bond strength. In a similar study, Ismail et al. [22] also noted that the presence of H^+ could destroy the alumino-silicate network of geopolymer materials and eventually lead to disintegration of the polymer gel. The findings of Lloyd et al. [35] concluded that H_3O^+ and HSO_4^- ions from the sulfuric acid could diffuse into the gel phase, where H_3O^+ attacks the gel and severely damage the gel network. However, Fig 9(b) indicates that inclusion of 2% nano-silica in the fly ash only geopolymer reduced acid

aggravation due to its additional reaction products. The mechanisms involved in the process are related to mechanical percolation along with pore filling effects of nano-silica. It appears that the aluminosilicate gel of the mix with 2% nano-silica (FA-NS2, Fig. 9(b)) was more compact than that of the control mix (FA-NS0, Fig. 9(a)). Similar differences are also observed in the mixes of the other two series. This observation on the differences in microstructures is consistent with the less strength loss of the mixes with 2% nano-silica, as shown in Fig. 8. It suggests that the introduction of 2% nano-silica reduced the porosity and increased the acid resistance in terms of strength loss and disintegration of the microstructure. The dense microstructure formed by nano-silica provides resistance to the penetration of acidic ions reducing the extent of disintegration in the microstructure and eventual less strength loss.

The energy dispersive X-ray patterns for fly ash only, OPC and GGBFS blended fly ash based geopolymers without nano-silica are shown in Figs. 10(a) to 10(c). Notable traces of silicon, sodium, aluminium and calcium elements were observed in the EDX patterns of the OPC and GGBFS blended fly ash geopolymers. Presence of the first three elements is from the sodium aluminosilicate gel, whereas the calcium is from gypsum formed in OPC and GGFBS blended geopolymers. Strong peaks of calcium were observed in the OPC and GGBFS blended geopolymers without nano-silica (Figs. 10(b) and 10(c)). These phenomena agreed well with the studies reported by other researchers [35, 41] that the exchanged calcium ions diffusing toward the acid solution react with the counter-diffusing sulfate anions resulting in the formation and deposition of gypsum crystals inside the corroding layer. The XRD patterns (Figs. 11(b) and 11(c)) also suggest a possible alteration and restructuring of the polymer network in the OPC and GGBFS blended geopolymers without nano-silica.

The XRD spectra of the samples after 90 days exposure to acid solution are shown in Figs. 11(a) to 11(c). It is confirmed from the XRD spectrum that the formation of gypsum takes place in both OPC and GGBFS blended fly ash geopolymers without nano-silica. The traces of gypsum are likely due to the reaction between available depleted calcium from the OPC and GGBFS with sulphur ions from the sulfuric acid. However, it is noted from Figs. 11(b) and 11(c) that the traces of gypsum entirely disappeared for both OPC and GGBFS blended geopolymers with 2% nano-silica. It seems Ca^{2+} that was released from the dissolution of OPC and GGBFS interacted with silicate ions and formed calcium silicate oligomers. However, no peaks of gypsum traces were observed for fly ash only geopolymers with and without nano-silica. Bakharev [20] and Lloyd et al. [32] noted that the acid resistance kinetics of polymer modified mortars depends on its material composition. In the

previous study [15] formation of aluminosilicate and CSH gel as final hydrated products were observed in GGBFS and OPC blended fly ash geopolymers. The presence of calcium silicate hydrate (CSH) in mixes FA-PC-NS0 and FA-S-NS0 might have reacted with H_2SO_4 and disintegrated in the form of calcium sulfate or as an amorphous silica gel at the end [39, 40]. Puertas et al. [41] and Wallah and Rangan [42] also concluded that the higher calcium content in the alkali activated binder generates greater amounts of gypsum during acidic exposure and might precipitate into and cover the pores of the mortar.

4. Conclusions

The effects of nano-silica on the flowability, compressive strength and acid resistance of ambient-cured geopolymer mortars were investigated. The geopolymer binders were based on fly ash alone or that blended with small proportions of GGBFS (15%) or OPC (10%).The following conclusions are drawn from the results obtained in this study:

- Inclusion of nano-silica improved the early-age strength of geopolymer mortars based on fly ash alone or that blended with OPC or GGBFS. Flow of the freshly mixed mortars gradually decreased with the increase of nano-silica because of its high specific surface. The compressive strength of the ambient-cured geopolymer mortars varied from 17 to 19 MPa at 7 days and from 29 to 60 MPa at 28 days. Strength development in ambient condition continued to the age of 90 days, however at slower rates after 56 days. The optimum dosage of nano-silica for maximum compressive strength was found to be 2% of the binder.
- Sorptivity of the specimens with 2% nano-silica was less than that of the control specimen. All the specimens remained intact after 90 days of immersion in 3% sulfuric acid solutions with some erosion on the surface of the specimens containing OPC. The average mass loss of the specimens of three series decreased from 2.6% to 1.8% after 90 days of immersion. The strength loss of the specimens without nano-silica ranged from 30% to 41% while that of the specimens with 2% nano-silica ranged from 9% to 11% after 90 days of immersion. Therefore, the acid resistance of geopolymer mortars significantly improved with the inclusion of 2% nano-silica.
- After 90 days of immersion in acid solutions, the microstructures of the specimens with nano-silica were found to be more compact as compared to the specimens without nano-silica. The combined effects of the nano-silica as a filler and enhanced reactivity of the aluminosilicate source materials refined the pore structure to develop a more compact microstructure. This reduced the porosity and sorptivity of the binder

matrix. As a result there was less damage in the matrix after immersion in acid solution and hence reduced loss of mass and strength in the specimen's containing nano-silica.

Acknowledgments

The authors wish to gratefully acknowledge the support of Coogee Chemicals for supplying the chemicals used in this study. The use of equipment, scientific and technical assistance of the Curtin University Electron Microscope facility, which has been partially funded by the university, State and Commonwealth Governments is also gratefully acknowledged.

Reference

1. Duxson P, Fernandez JA, Provis JL, Lukey GC, Palomo A, Deventer JSJ. Geopolymer technology: the current state of the art. J Mater Sci 2007; 42 (9): 2917–2933.
2. Khale D, Chaudhary R. Mechanism of Geopolymerization and Factors Influencing Its Development: A Review. J Mater Sci 2007; 42:729-746.
3. Deb P, Nath P, Sarker PK. The effects of ground granulated blast-furnace slag blending with fly ash and activator content on the workability and strength properties of geopolymer concrete cured at ambient temperature. Mater Design 2014; 62: 32-39.
4. Deb PS, Nath P, Sarker PK. Strength and Permeation Properties of Slag Blended Fly Ash Based Geopolymer Concrete. Adv Mater Res 2013; 651:168-173.
5. Rahman MM, Sarker PK. Geopolymer concrete columns under combined axial load and biaxial bending. Concrete 2011: 25thBienniel Conference of the Concrete Institute of Australia: Western Australia, 2011.
6. Fernandez JA, Torre AG, Palomo A, Olmo GL, Alonso MM, Aranda MAG. Alkali Activated Materials. Fuel 2006; 85:625–634.
7. Diaz EI, Allouche EN, Eklund S. Factors affecting the suitability of fly ash as source material for geopolymers. Fuel 2010; 89: 992–996.
8. Nath P, Sarker PK. Effect of GGBFS on setting, workability and early strength properties of fly ash geopolymer concrete cured in ambient condition. Constr Build Mater 2014; 66:163–171.
9. Nath P, Sarker PK. Use of OPC to improve setting and early strength properties of low calcium fly ash geopolymer concrete cured at room temperature. Cement Concrete Comp 2015; 55: 205–214.
10. Quercia G, Spiesz P, Hüsken G, Brouwers HJH. SCC modification by use of amorphous nano-silica. Cement Concrete Comp 2014; 45: 69–81.

11. Senff L, Hotza D, Repette WL, Ferreira VM, Labrincha JA. Mortars with nano-SiO2 and micro-SiO2 investigated by experimental design. Constr Build Mater 2010; 24(8):1432-1437.
12. Jalal M, Mansouri E, Sharifi M, Pouladkhan AR. Mechanical, rheological, durability and microstructural properties of high performance self-compacting concrete containing SiO2 micro and nanoparticles. Mater Design 2012; 34:389–400.
13. Parida SK, Dash S, Patel S, Mishra BK. Adsorption of organic molecules on silica surface. Advan in Colloid and Interf Scie 2006; 121:77–110.
14. Sobolev K, Flores I, Torres MLM, Valdez PL, Zarazua E, Cuellar EL. Engineering of SiO_2 nanoparticles for optimal performance in nano cement based materials. Nanotech Constr 3. Spring 2009; 139–48.
15. Deb PS, Sarker PK, Barbhuiya S. Effects of nano-silica on the strength development of geopolymer cured at room temperature. Constr Build Mater 2015; 10(1): 675–683.
16. Adak D, Sarkar M, Mandal S. Effect of nano-silica on strength and durability of fly ash based geopolymer mortar. Constr Build Mater 2014;70: 453–459
17. Gao X, Yu QL, Brouwers HJH. Characterization of alkali activated slag–fly ash blends containing nano-silica. Constr Build Mater 2015;98: 397–406
18. Mehta PK. Studies on chemical resistance of low water/cement ratio concrete. Cement Concrete Res 1985; 15: 969.
19. Chindaprasirt P, Paisitsrisawat P, Rattanasak U. Strength and resistance to sulfate and sulfuric acid of ground fluidized bed combustion fly ash–silica fume alkali-activated composite. Adv Powder Technol 2014; 25:1087–1093.
20. Bakharev T. Resistance of geopolymer materials to acid attack. Cement Concrete Res 2005; 35: 658–670.
21. Breck DW. Zeolite Molecular Sieves: Structure, Chemistry and Use. New York: Wiley-Inter science, 1974. p. 415–418.
22. Ismail I, Bernal SA, Provis JL, Hamdan S, Deventer JSJ. Microstructural changes in alkali activated fly ash/slag geopolymers with sulfate exposure. Mater Struct 2013; 46: 361–373.
23. American Society of testing materials. Standard Test Method for Flow of Hydraulic Cement Mortar. ASTM C1437-13
24. American Society of testing materials. Standard Test Method for Compressive Strength of Hydraulic Cement Mortars (Using 2-in. or [50-mm] Cube Specimens), ASTM C109/C109M; 2002.

25. American Society of testing materials. Standard Test Methods for Chemical Resistance of Mortars, Grouts, and Monolithic Surfacings and Polymer Concretes. ASTM C 267
26. American Society of testing materials. Standard test method for measurement of rate of absorption of water by hydraulic-cement concretes. ASTM C1585-13.
27. Provis JL, Duxson P, Deventer JSJ. The role of particle technology in developing sustainable construction materials. Adv Powder Technol 2010; 21:2–7.
28. Fernandez JA, Palomo A. Characterisation of fly ashes. Potential reactivity as alkaline cements. Fuel 2003; 82: 2259–2265.
29. Temuujin J, Williams RP, Riessen A. Effect of mechanical activation of fly ash on the properties of geopolymer cured at ambient temperature. J Mater Proces Tech 2009; 209: 5276–5280.
30. Fernandez JA, Monzo M, Vicent M , Barba A, Palomo A. Alkaline activation of metakaolin–fly ash mixtures: Obtain of Zeoceramics and Zeocements. Micropor Mesopor Mat 2008; 108:41–49.
31. Belkowitz JS, Belkowitz WB, Nawrocki K, Fisher FT. the impact of nano silica size and surface area on concrete properties. Mater J 2015; 112:419-428.
32. Chindaprasirt P, Jaturapitakkul C, Sinsiri T. Effect of fly ash fineness on microstructure of blended cement paste. Constr Build Mater 2007; 21:1534–41.
33. Somna K, Jaturapitakkul C, Kajitvichyanukul P, Chindaprasirt P. NaOH- activated ground fly ash geopolymer cured at ambient temperature. Fuel 2011; 90(6):2118–24
34. Law DW, Adam AA, Patnaikuni I, Molyneaux TK, Wardhono A. Long term durability properties of class F fly ash geopolymer concrete. Mater Struct 2015; 48:721–731.
35. Lloyd RR, Provis JL, Deventer JSJ. Acid resistance of inorganic polymer binders. 1. Corrosion rate. Mater Struct 2012; 45:1–14.
36. Fattuhi N, Hughes B, The performance of cement paste and concrete subjected to sulphuric acid attack. Cement Concrete Res 1988; 18 (4):545–553.
37. Israel D, Macphee DE, Lachowsk EE. Acid attack on pore-reduced cements. J Mater Sci 1997; 32:4109-4116.
38. Chindaprasirt P, Taebuanhuad S, Rattanasak U. Resistance to acid and sulfate solutions of microwave-assisted high calcium fly ash geopolymer. Mater Struct 2013; 46:375–381.
39. Hartman RL, Fogler HS. Understanding the dissolution of zeolites. Langmuir 2007; 23(10):5477–5484

40. Allahverdi A, Skavara F. Sulfuric acid attack on hardened paste of geopolymer cements. Part 1. Mechanism of corrosion at relatively high Concentrations. Ceram-Silikaty 2001; 45(3): 81-88
41. Puertas F, Mejía GR, Fernández JA, Delvasto S, Maldonado J. Alkaline cement mortars. Chemical resistance to sulfate and seawater attack. Mater Construcc 2002; 52:55–71.
42. Wallah SE, Rangan BV. Low Calcium Fly Ash Based Geopolymer Concrete: Long Term Properties". Research Report GC2, Faculty of Engineering, Curtin University of Technology, Perth, Australia.2006: 01-97.

Table 1. Chemical compositions of fly ash, OPC and GGBFS (% mass)

Material	SiO_2	Al_2O_3	Fe_2O_3	CaO	MgO	MnO	K_2O	Na_2O	P_2O_5	TiO_2	SO_3	LOI[a]
Fly ash	46.69	29.14	13.81	3.29	1.4	0.16	0.72	0.86	1.63	1.34	0.43	-
OPC	21.1	4.7	2.7	63.6	2.6	-	-	-	-	-	2.5	2
GGBFS	29.96	12.25	0.52	45.45	-	-	0.38	0.31	0.04	0.46	3.62	2.39
Nano-silica	99.5	0.001	0.001	-	-	-	-	-	-	-	-	-

[a] Loss on ignition

Table 2. Mix proportions of geopolymer mortars (Kg/m^3)

Mix	Fly ash only				OPC blended Fly ash				GGBFS blended Fly ash			
ID	FA-NS0	FA-NS1	FA-NS2	FA-NS3	FA-PC-NS0	FA-PC-NS1	FA-PC-NS2	FA-PC-NS3	FA-S-NS0	FA-S-NS1	FA-S-NS2	FA-S-NS3
Sand	1173	1173	1173	1173	1173	1173	1173	1173	1173	1173	1173	1173
Fly ash	734	726	718	711	660	652.67	645.33	638.00	623.33	616.00	608.67	601.33
GGBFS	-	-	-	-	-	-	-	-	110.00	110.00	110.00	110.00
OPC	-	-	-	-	73.33	73.33	73.33	73.33	-	-	-	-
SH[a]	97.78	97.78	97.78	97.78	97.78	97.78	97.78	97.78	97.78	97.78	97.78	97.78
SS[b]	195.56	195.56	195.56	195.56	195.56	195.56	195.56	195.56	195.56	195.56	195.56	195.56
Nano silica	-	7.33	14.67	22.00	-	7.33	14.67	22.00	-	7.33	14.67	22.00

[a]Sodium hydroxide, [b]Sodium silicate

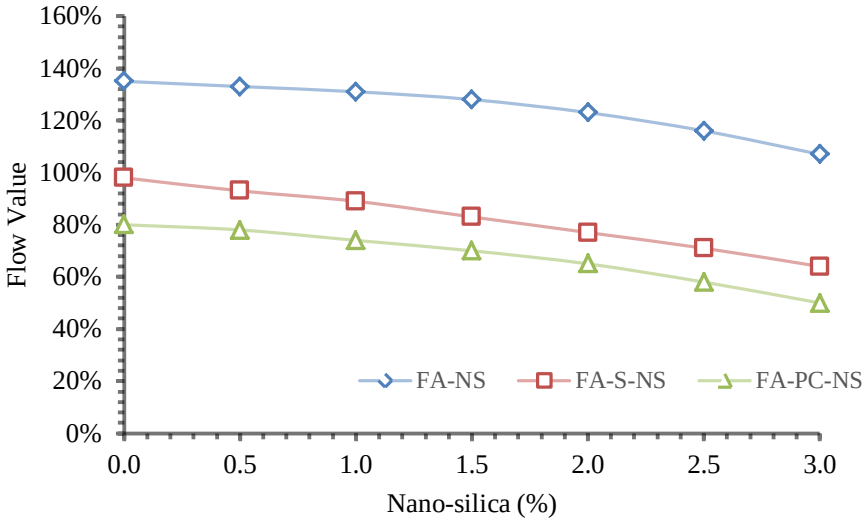

Fig. 1. Change in flow of geopolymer mortars with nano-silica.

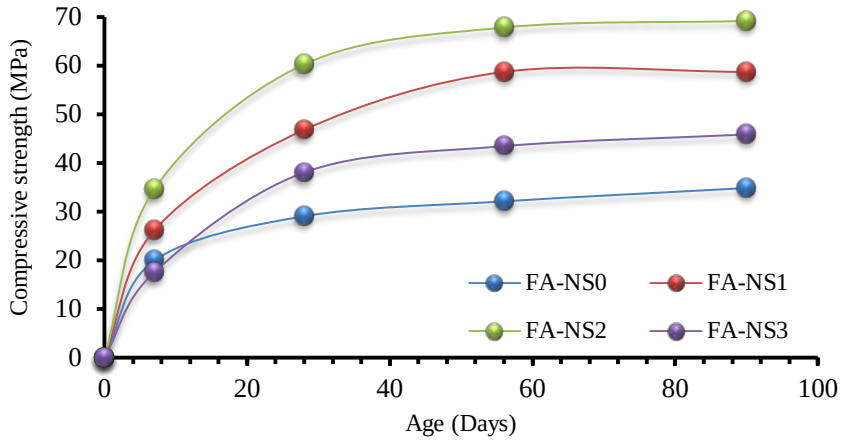

Fig. 2. Strength development of fly ash based geopolymer mortars with nano-silica

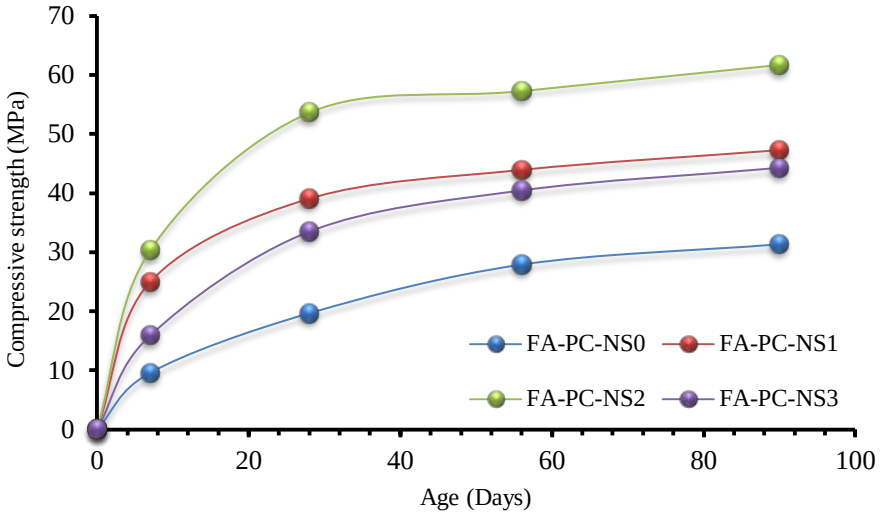

Fig. 3. Strength development of OPC blended fly ash based geopolymer mortar with nano-silica

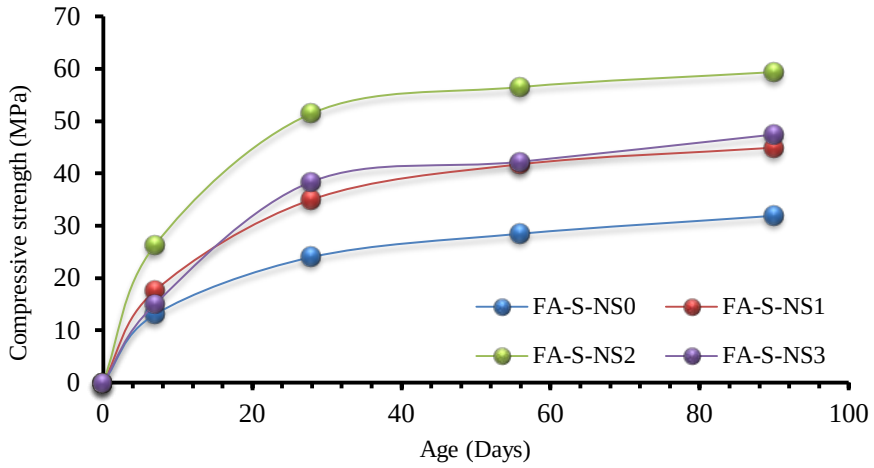

Fig. 4. Strength development of GGBFS blended fly ash based geopolymer mortar with nano-silica

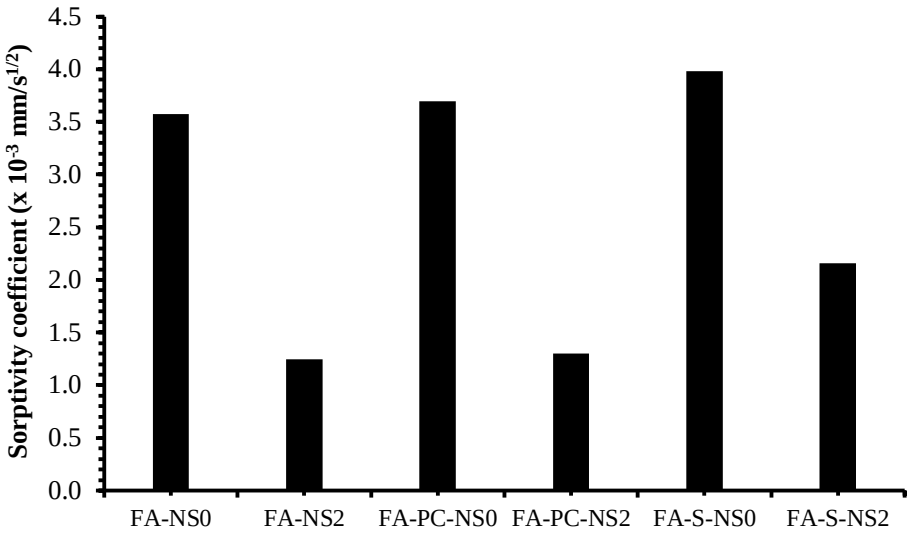

Fig. 5. Sorptivity coefficient of geopolymer mortars with nano-silica.

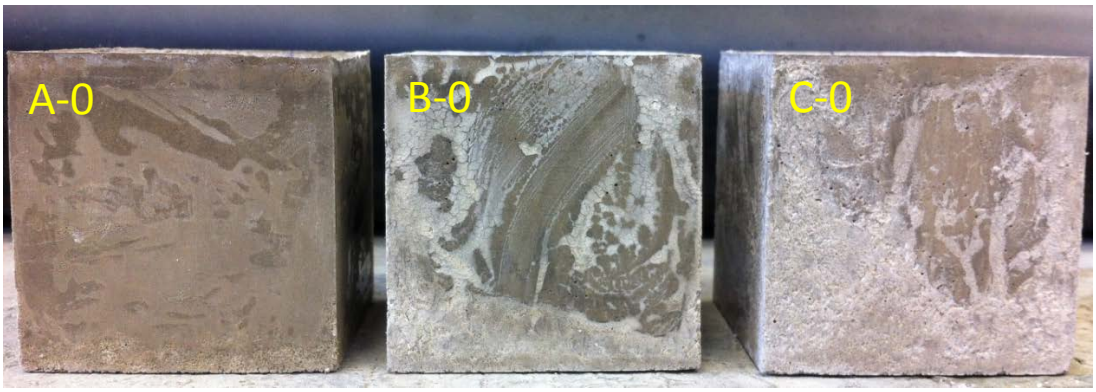

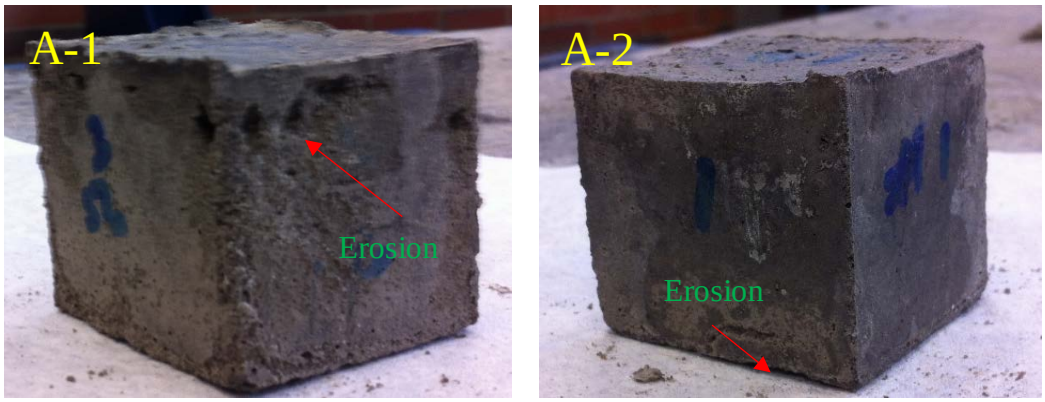

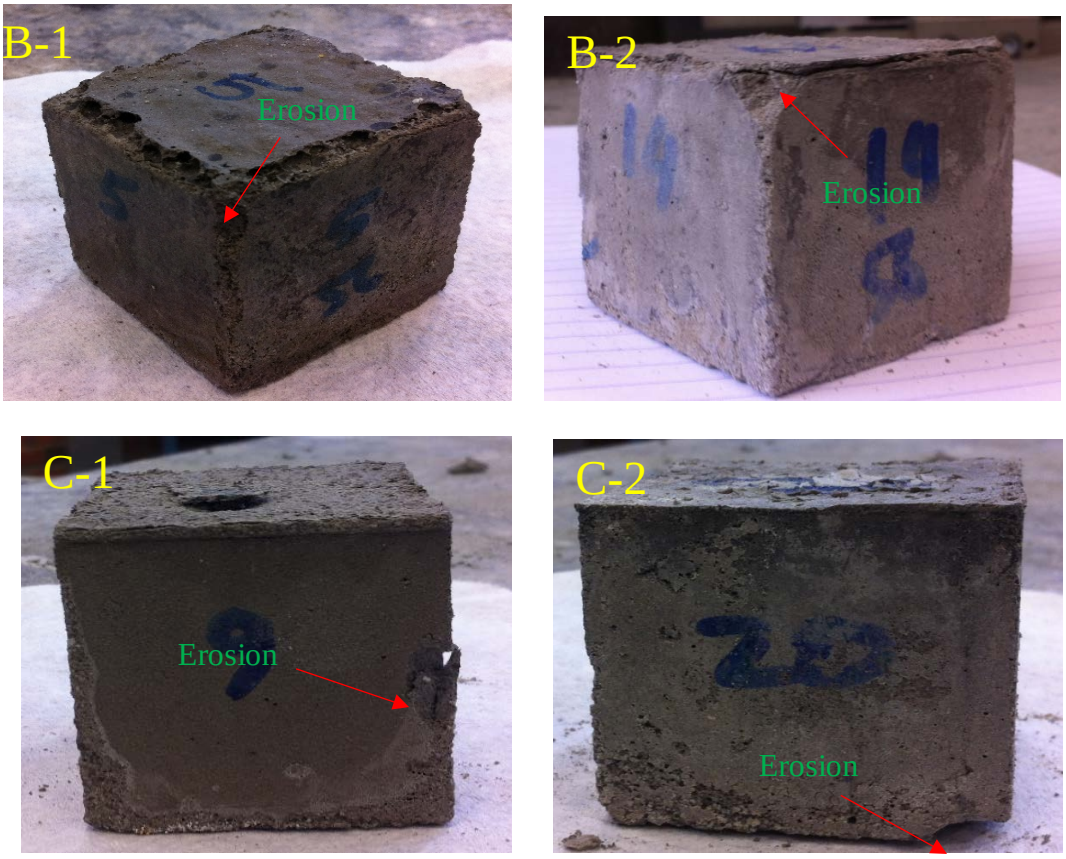

Fig. 6. Visual appearance of geopolymer specimens before acid submerged (A-0: FA-NS0, B-0: FA-PC-NS0, C-0: FA-S-NS0) and after 90 days acid exposure (A) A-1: FA-NS0, A-2: FA-NS2 (B) B-1: FA-PC-NS0, B-2: FA-PC-NS2, (C) C-1: FA-S-NS0, C-2: FA-SNS2.

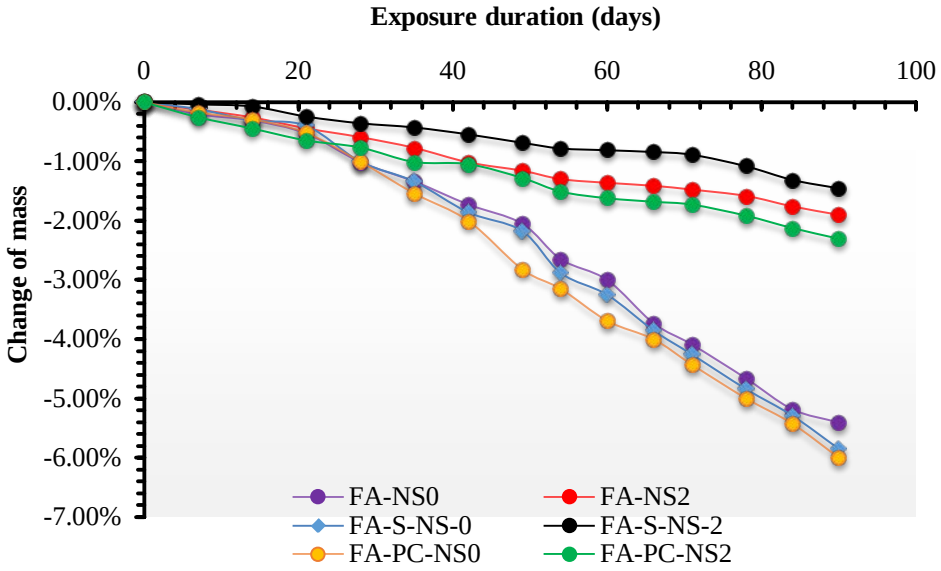

Fig. 7. Change in mass of mortar specimens after immersion in 3% sulfuric acid solution.

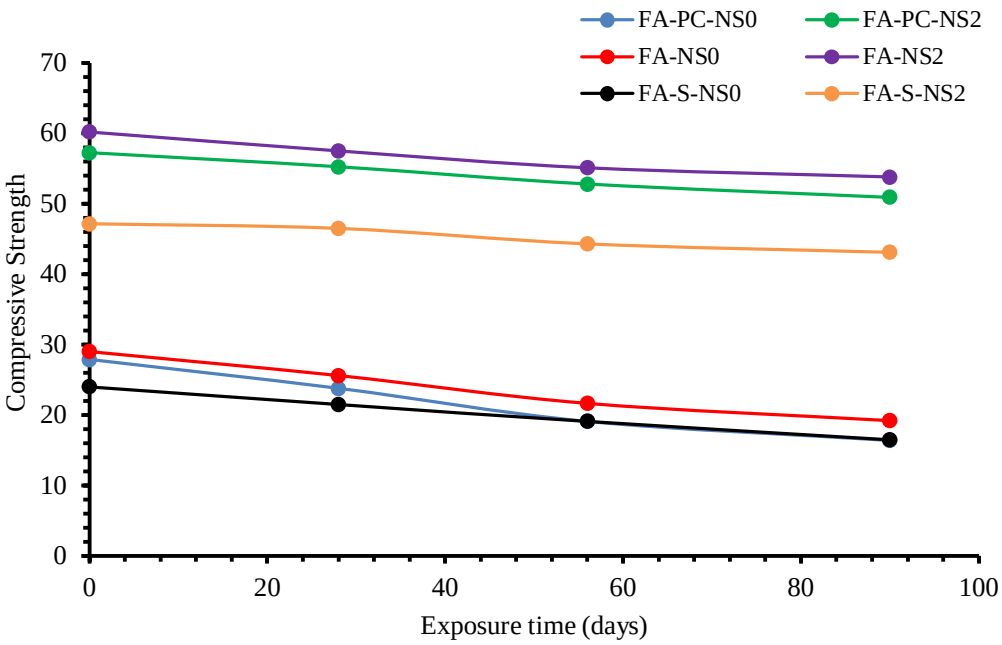

561
562 **Fig. 8.** Change in compressive strength of geopolymer mortars in sulfuric acid exposure.

563

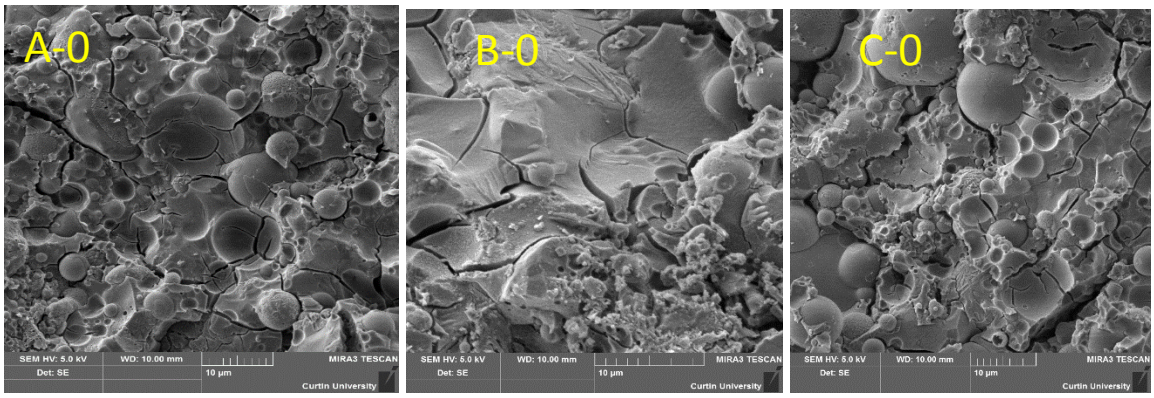

564

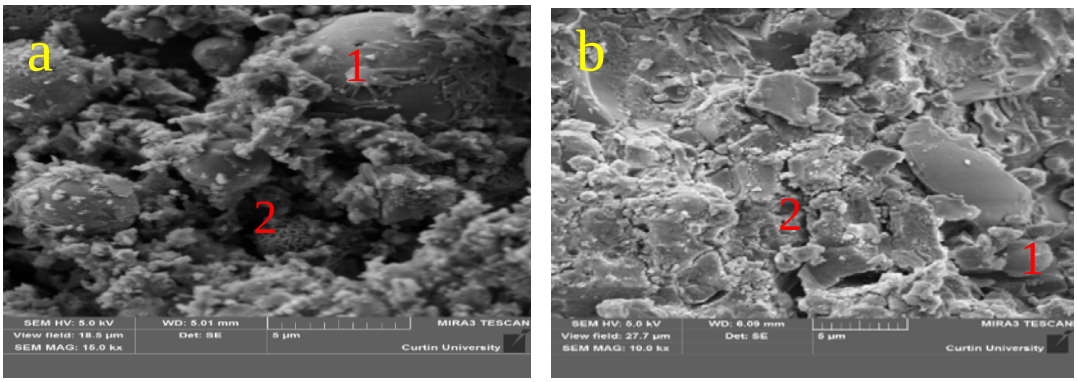

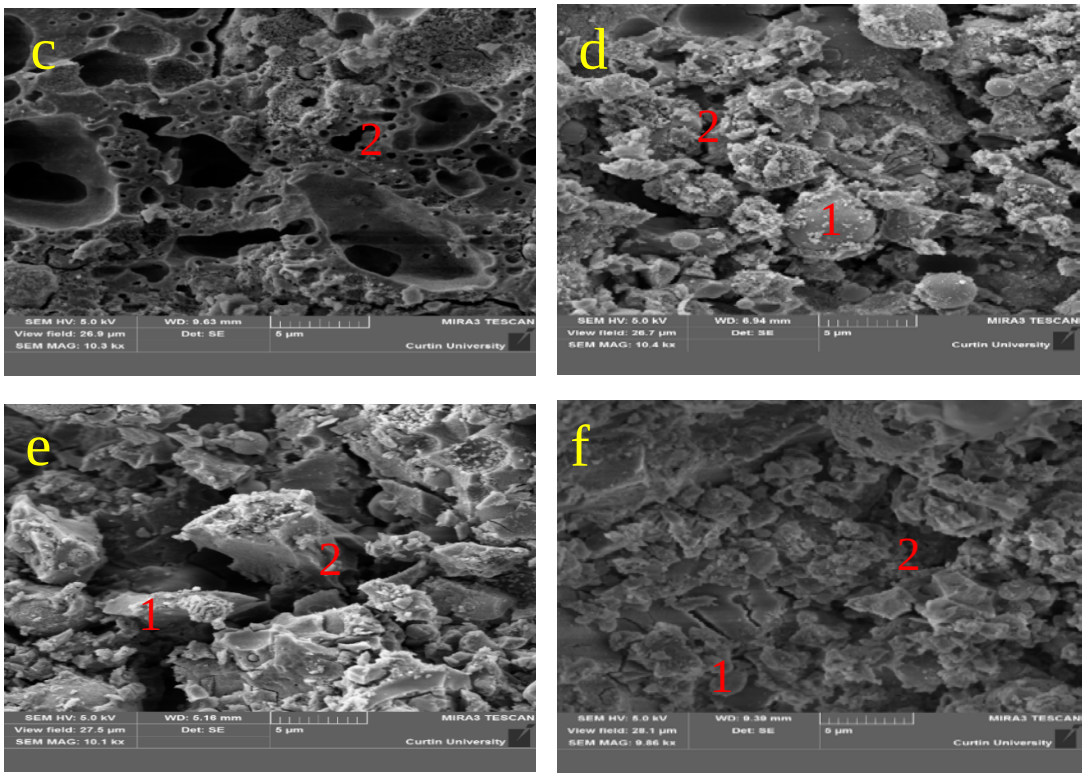

Fig. 9. SEM images of geopolymer mortars before acid submerged (A-0: FA-NS2, B-0: FA-PC-NS2, C-0: FA-S-NS2) and after 90 days acid exposure (a) FA-NS0, (b) FA-NS2, (c) FA-PC-NS0, (d) FA-PC-NS2, (e) FA-S-NS0 and (f) FA-S-NS2

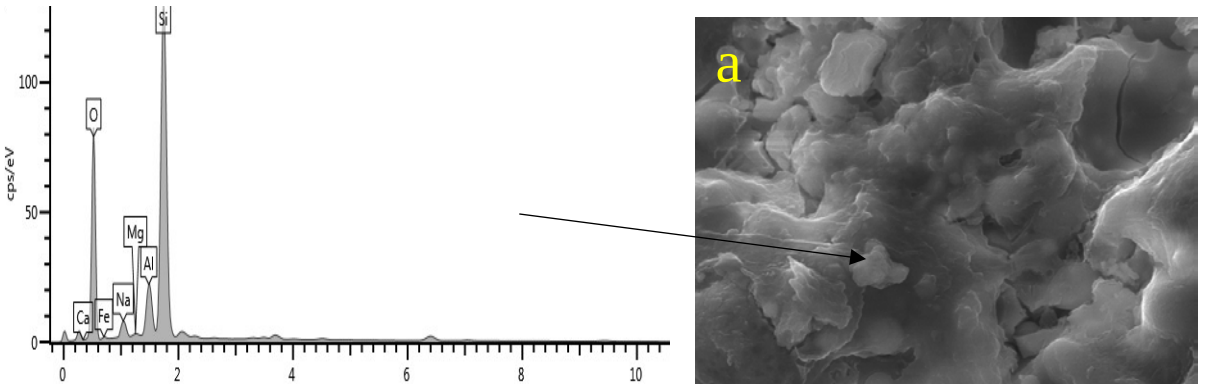

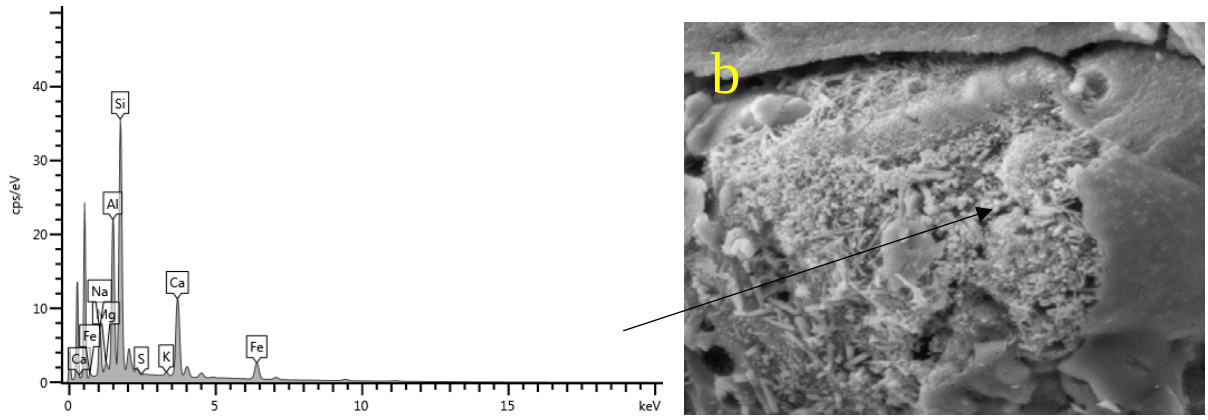

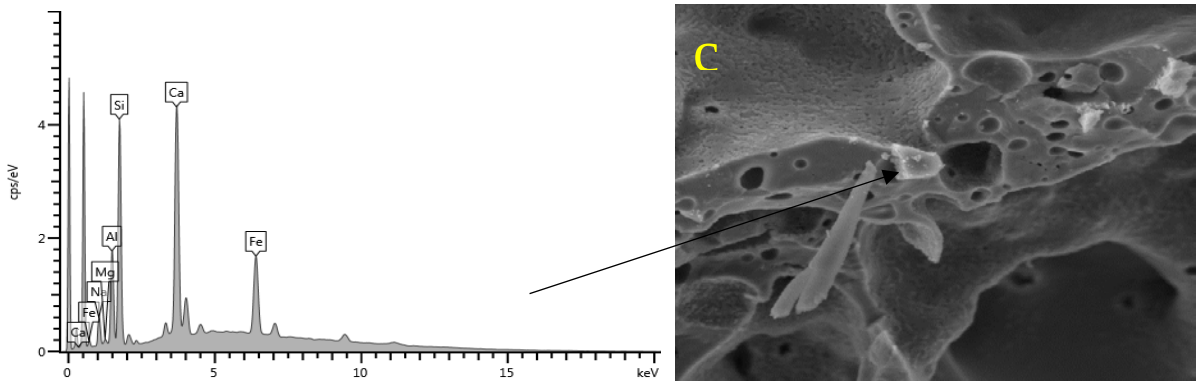

574

575 **Fig.10.** EDX spectra of geopolymers mortar without nano-silica under acid exposure (a) Fly-
576 ash only, (b) OPC blended fly-ash and (c) GGBFS blended fly-ash

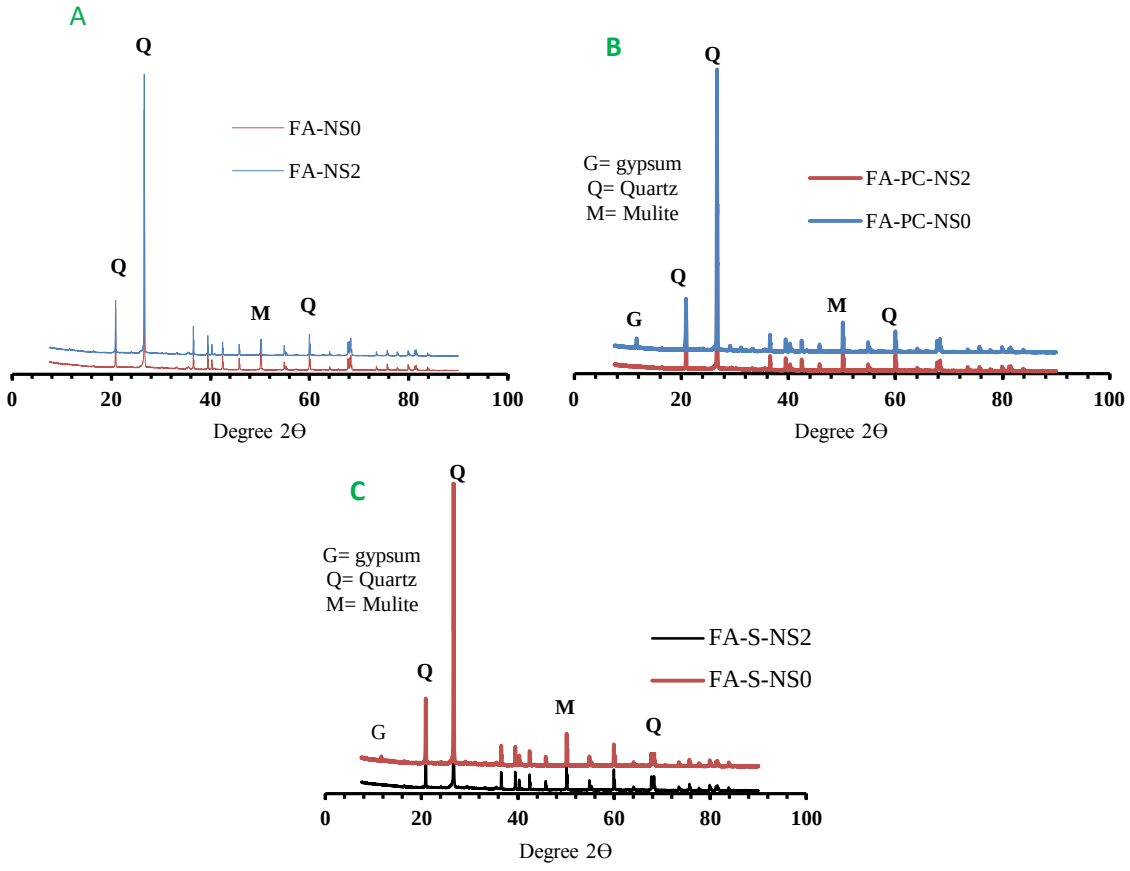

577

578

579 **Fig. 11.** X-ray diffraction patterns of geopolymers mortar under sulfuric acid exposure: (A)
580 fly ash only with 0% and 2% nano-silica. (B) OPC blended fly ash with 0% and 2% nano-
581 silica (C) GGBFS blended fly ash with 0% and 2% nano-silica.
582
583
584
585
586
587
588

589